Correlation of the precursor type with densification behavior and microstructure of sintered mullite ceramics

Hrvoje Ivankovic[a], Emilija Tkalcec[a,*], Ruediger Nass[b], Helmut Schmidt[b]

[a]*Faculty of Chemical Engineering and Technology, University of Zagreb, 19 Marulicev trg, PO Box 177, HR 10000 Zagreb, Croatia*
[b]*Institut fuer Neue Materialien, Im Stadtwald, Gebaeude 43, D 66123 Saarbruecken, Germany*

Abstract

The effect of alumina component in diphasic mullite precursors containing alkoxy derived silica on the crystallization and sintering behavior of compacts was studied. The phenomena observed were characterized using differential thermal analysis (DTA), powder X ray diffraction (XRD), dilatometry and transmission and scanning electron microscopy (TEM, SEM). In order to change the characteristics of as prepared gels, the alumina source was varied while keeping the silica source constant. $Al(NO_3)_3{\cdot}9H_2O$, γ Al_2O_3 and boehmite (γ AlOOH) were used as the alumina source and TEOS as the silica source. Clear differences were found in the microstructure of sintered samples derived from the precursors with aluminum nitrate nonahydrate in comparison to the samples containing γ Al_2O_3 or boehmite (γ AlOOH). The former exhibited elongated mullite grains embedded into the ''equiaxial mullite matrix''. This morphology is due to the overlapping of mullite crystallization and viscous flow sintering temperatures. Transient alumina, either added as γ Al_2O_3 or formed in situ by decomposition of boehmite, shifts the mullite formation above the sintering temperature, and enables formation of equiaxial mullite. The smaller are the transient alumina particles, the smaller are mullite grains of sintered bodies.

Keywords: Grain size; Microstructure; Mullite; Sintering; Sol gel processes

1. Introduction

Although extensive work has been done related to the processing and characterization of sol-gel derived materials having mullite compositions, ($Al^{VI}[Al^{IV}_{2+2x}Si_{2-2x}O_{10-x}]$ where $0.22 < x < 0.58$),[1] a complete understanding in terms of the relationship between the initial process parameters and the sintering behavior and microstructure of mullite ceramics has not yet been fully achieved.

The general agreement is that the mixing scale in mullite sol-gel precursors actually controls the phase transformation sequence and the temperature of mullite formation as well as the properties of sintered bodies.[2]

Different types of mullite precursors were described depending on the degree of homogeneity in as-prepared powders.[2–8] Single-phase mullite precursors, or type I precursors (Schneider's definition[2]) possess atomic or near atomic level of homogeneity and transform into tetragonal/or pseudotetragonal mullite at ~980 °C. In gels with nanometer scale of homogeneity (diphasic gels), however, two different pathways of phase development are observed. Diphasic gels designated by Schneider as type II precursors consist of pseudo-boehmite and amorphous silica at room temperature. It is generally accepted that the transformation of pseudo-boehmite follows the same phase transformation sequence as that in boehmite forming γ-Al_2O_3, which transforms in δ-Al_2O_3. The latter phase reacts with amorphous silica forming mullite above 1250 °C. Diphasic gels designated as types III precursors are non-crystalline up to about 980 °C and mullite formation is preceded by the formation of a weak crystalline transient alumina such as cubic Al–Si spinel or γ-Al_2O_3 at 980 °C, which later reacts with amorphous silica forming mullite at temperatures lower than 1250 °C. However, most mullite gels consist of a combination of

* Corresponding author. Fax: +385 1 4597 250.
E mail address: etkalcec@pierre.fkit.hr (E. Tkalcec).

different types of precursors, rather than that of the intended end members.[7]

The effect of varying the scale of mixing on the densification and microstructure of mullite ceramics has been investigated in several studies.[8–12] Single-phase mullite precursors do not sinter effectively without the application of high temperatures and/or high pressures. In contrast, mullite prepared from colloidal precursors can be sintered at much lower temperatures. Another way to achieve dense mullite ceramics at lower temperatures is a technique involving transient viscous sintering of microcomposites consisting of alumina particles coated with an amorphous silica layer. Sacks et al.[13,14] achieved dense ceramics by sintering of α-Al_2O_3 particles coated with an amorphous silica at 1600 °C. Bartsch et al.[15] reduced processing temperatures by ≈300 °C with amorphous SiO_2-coated γ-Al_2O_3 instead of α-Al_2O_3 particles. They pointed out that improved densification at lower temperatures is due to transient viscous flow sintering of amorphous silica.

The aim of this work was to study the influence of Al_2O_3 component (its crystalline form and particle size) on the crystallization pathway of diphasic gels containing alkoxy derived silica, and on the sintering behavior of compacted precursors. As alumina components used were: $Al(NO_3)_3{\cdot}9H_2O$, γ-Al_2O_3 and boehmite (γ-AlOOH). Special attention was given to differentiate the crystallization path and the microstructure of sintered bodies when precursors containing boehmite or in situ formed pseudoboehmite were used. The structural evolution with temperature has been studied by differential thermal analysis (DTA) and X-ray diffraction (XRD). The microstructure and morphology of sintered ceramics has been investigated by scanning and transmission electron microscopy (SEM, TEM) and energy dispersive X-ray spectrometry (EDX).

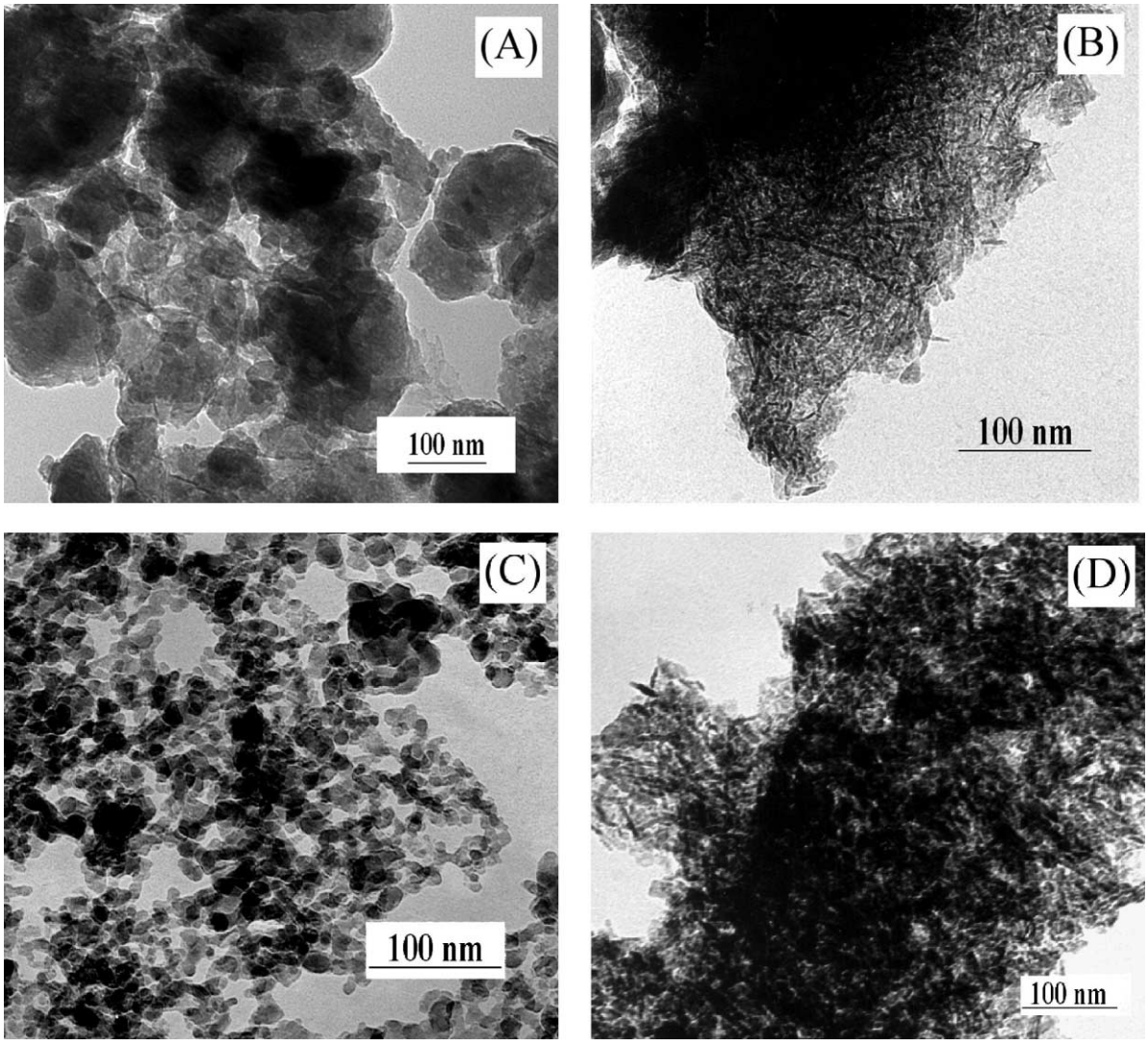

Fig. 1. TEM micrographs of prepared and dried precursors: (A) gel *A*, (B) gel *B*, (C) a water suspension of γ Al_2O_3 just before TEOS was added to prepare the gel *C*, and (D) gel *D*.

2. Experimental procedure

2.1. Gel preparation

Four precursors with the stoichiometric mullite composition ($3Al_2O_3{\cdot}2SiO_2$) but with different level of mixing were prepared as follows: The gel *A* was prepared by dissolving $Al(NO_3)_3{\cdot}9H_2O$ in water (nitrate/water molar ratio equals 1:32). The solution was stirred and refluxed at 60 °C overnight. Tetraethylsilane (TEOS, Fluka >98%) previously mixed with ethanol (with TEOS/ethanol molar ratio of 1/4) was added dropwise to the nitrate solution. The mixture was heated at 60 °C under reflux condition until gelation (8 days). For the preparation of the gel *B* the same procedure was used, but $Al(NO_3)_3{\circ}9H_2O$ was dissolved in ethanol and after mixing the solutions (nitrate and TEOS) the stirring was continued for next 12 h whereupon the mixture was brought to pH 6 by adding 2M aqueous ammonia. Gels *C* and *D* were synthesized from γ-Al_2O_3 ("Aluminium oxide C", Degusa, 15 nm mean particle size, specific surface area of 100 $m^2\ g^{-1}$) and γ-AlOOH, boehmite, ("Disperal" Condea Chemie, specific surface area of 188 $m^2\ g^{-1}$), respectively. Both powders were peptizied by adding 0.1 M HNO_3 in a concentration of 10%. The suspensions were then stirred and refluxed for 24 h at 60 °C. Stoichiometric amount of tetraethoxysilane (TEOS, Fluka >98%) in ethanol was dropwise added and gelation was carried out by refluxion at 60 °C. All prepared gels were further dried at 110 °C for 72 h and were stored in a vacuum desiccator.

2.2. Characterization methods

The dried gels were characterized using differential thermal analysis (DTA). DTA of mullite precursors were performed on thermoanalyser Netzsch Model 409 under the constant synthetic air flow of 75 $cm^3\ min^{-1}$, at the heating rate of 5 °C min^{-1}. To establish the sequence of crystallization, heating in DTA apparatus was stopped successively at different temperatures. The samples were held at the end temperature for 2 h and analyzed by X-ray diffraction analysis.

XRD was carried out on a computer controlled diffractometer (Siemens D500/PSD) using CuK_α radiation with a quartz single-crystal monochromator, and a curved position sensitive detector. Data were collected between 5 and 70° 2θ in step scan mode with the step of 0.02° and counting time of 3 s/step.

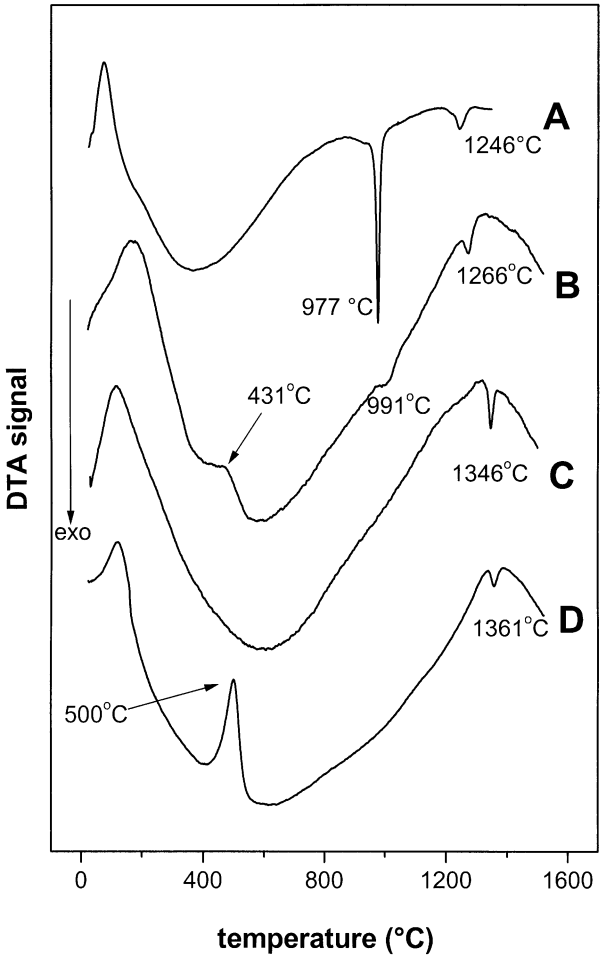

Fig. 2. DTA scans of prepared precursors at a heating rate of 5 °C min^{-1}. The sample notations are explained in Table 1.

Table 1
Designation of the as prepared and dried gels

Gel	Type of gels[a]	Al precursor/solvent	Si precursor/solvent	SSAs B.E.T ($m^2\ g^{-1}$)	EDX analysis Al_2O_3/SiO_2 (wt.%)
A	Diphasic, type III	$Al(NO_3)_3{\cdot}9H_2O$/water	TEOS/EtOH	187	72.0/28.0
B	Diphasic[b] (combination of type II and type III)	$Al(NO_3)_3{\cdot}9H_2O$/EtOH + NH_4OH (pseudoboehmite)	TEOS/EtOH	262	72.1/27.9
C	Diphasic, type II[c]	γ Al_2O_3/water	TEOS/EtOH	208	71.7/28.3
D	Diphasic, type II[c]	Boehmite/water	TEOS/EtOH	233	72.1/27.9

[a] Clasification according to Schneider.[2]
[b] NH_4OH solution is added to adjust pH to 6.
[c] The gels can be considered as amorphous SiO_2 coated γ Al_2O_3 nanocomposites.

The specific surface area (SSAs) of dry and milled precursors were measured at −196 °C using a sorption analyser (Model ASAP Micromeritics Instrument Corp.) with N_2 as the adsorbate gas. Prior to analysis samples were degassed at 120 °C. SSAs were calculated using Brunauer–Emmett–Teller (B.E.T) multipoint method. The gels were calcined at 700 °C for 9 h to decompose organics and to remove volatiles before preparing the pellets for dilatometric analysis and for studying the sintering of gels. The shrinkage behavior of the compacts was examined from room temperature up to 1600 °C at the heating rate of 5 °C min^{-1} using a difference Linseis dilatometer with an Al_2O_3 measurement system. Green compacts of $\phi = 5$ mm, $L = 10$ mm and $\phi = 10$ mm, $L = 10$ mm, respectively, were prepared by uniaxial (100 MPa), followed by isostatic pressing at 200 MPa. The former compacts were used for dilatometric measurements and the latter for observation of sintering behavior and microstructure of the sintered bodies. The density of compacts was examined from room temperature up to 1650 °C at the heating rates of 5 °C min^{-1} with 2 h hold at the end temperature. Bulk densities of compacts were measured by the Archimedes method with distilled water as immersion liquid. The relative densities were calculated using the theoretical density of mullite (3.17 g cm^{-3}, JCPDS-card No. 15-776).

Dry-gel morphologies were examined using transmission electron microscopy (TEM) (JEOL 6400 F). Microstructure observations and microanalysis of sintered bodies were performed by scanning electron microscope (SEM) and energy dispersive X-ray analyser (EDX) (JEOL 6400 F). For microstructure observation, the sintered compacts were polished with 1 μm diamond paste and thermally etched at 1450 °C for 30 min.

3. Results

TEM micrographs of dried gels *A*, *B* and *D* are shown in Fig. 1 along with the micrograph of γ-Al_2O_3 suspension. It is interesting to note that γ-Al_2O_3 in the as-prepared precursor *C* was not visible in TEM micrograph, although the XRD pattern confirmed it at room temperature. Therefore, its particle size was measured in the suspension just before TEOS was added. The EDX and

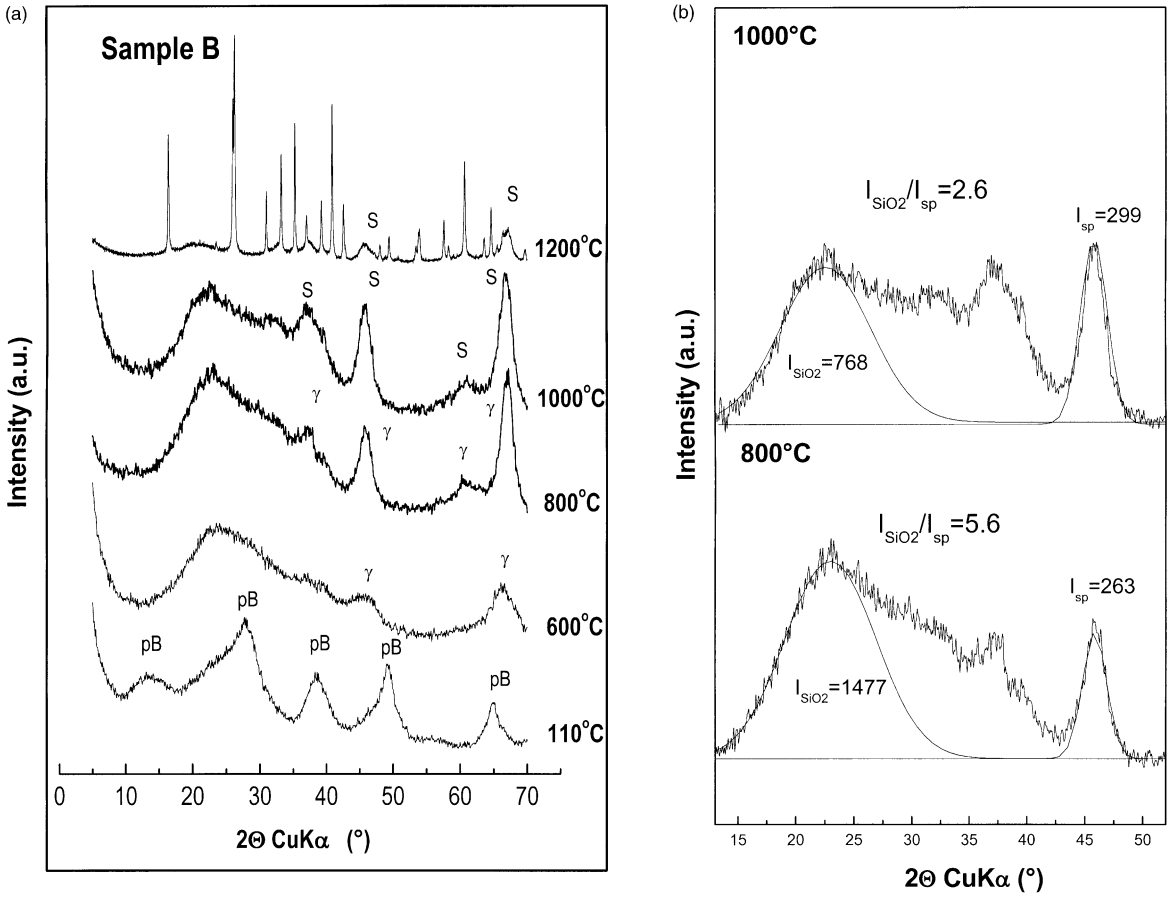

Fig. 3. (a) XRD patterns of the sample *B* heated in DTA up to the temperatures given in the picture. pB pseudoboehmite, γ γ Al_2O_3 and S (both phases; γ Al_2O_3 and Al Si spinel. (b) intensity ratios of amorphous SiO_2 hump at 22° 2θ CuK_α (I_{SiO2}) and spinel line at 2θ 45.6° (I_{sp}) at 800 and 1000 °C, respectively. Full lines are the best fit of the corresponding intensities. Mullite peaks are not marked.

B.E.T analyses of the gels are given in Table 1. The compositions of gels were measured at 10 different positions and the mean value is presented in the table. DTA scans of prepared precursors dried at 110 °C are shown in Fig. 2, and the corresponding XRD patterns of samples heated in DTA apparatus up to different temperatures in Figs. 3–5. In Figs. 3b and 5b the area below the amorphous silica hump at 22° 2θ CuK_α was compared with the area of spinel at $2\theta \mathrm{Cu}K_\alpha = 45.6°$ for the samples *B* and *D* at two different temperatures.

In Fig. 6a and b the length changes ($\Delta L/L$) and the corresponding derivative curves, $\mathrm{d}(\Delta L/L)\mathrm{d}T$, at the heating rates of 5 °C min^{-1} are shown. The gels *A* and *B* exhibit three steps of densification; the gel *D* exhibits only one large densification step between 1000 and 1300 °C, while the gel *C* exhibits a large step between 1000 and 1300 °C, and a second smaller step above 1360 °C.

Bulk densities after pressureless sintering as a function of temperature between 1450 and 1650 °C are shown in Fig. 7. The holding time at each temperature was 2 h. Fig. 8 shows representative SEM micrographs of polished and thermally etched pressureless sintered compacts at 1600 °C. TEM micrograph of the sample *C* (alumina component was added as γ-Al_2O_3) isothermally sintered at 1320 °C for 4 h is given in Fig. 9.

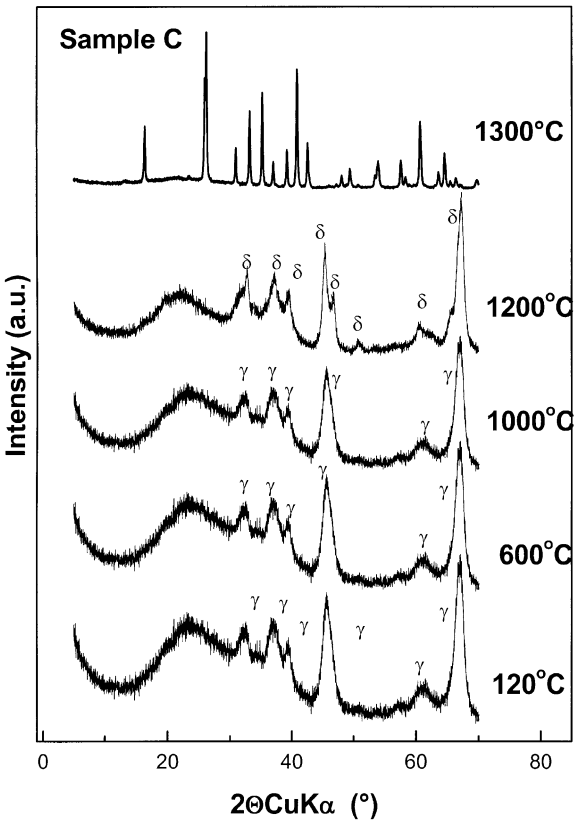

Fig. 4. XRD patterns of the sample *C* heated in DTA up to the tem peratures given in the picture. γ γ Al_2O_3, δ δ Al_2O_3. Mullite peaks are not marked.

4. Discussion

4.1. Powder characterization

Depending on the starting materials and the methods applied (Table 1), the synthesized precursors have different properties, which in turn affect the resulting properties of the ceramics. All four gels have the same 3:2 mullite composition (within the error span of EDX analysis) and similar specific surface area. However, the as-dried gel *A* is amorphous at room temperature, while in the other three gels alumina component is present in a crystalline form; as pseudoboehmite in the sample *B*, γ-Al_2O_3 in the sample *C*, and boehmite in the sample *D*. The size of alumina component in gels increases from 10 nm (sample *B*), through 20 nm (sample *C*) to 30–40 nm (sample *D*) as shown in TEM micrographs in Fig. 1. XRD analysis reveals that gel *A* is amorphous up to the first exotherm at 977 °C seen on DTA scan (Fig. 2). After this point the XRD pattern displays only weakly crystallized spinel phase (γ-Al_2O_3 or Al–Si spinel), which reacts with amorphous silica at about 1246 °C forming orthorhombic mullite. The mullite formation in the gel *A* is typical for type III gels, therefore, the corresponding XRD patterns are not presented here. The crystallization pathway of the sample *B* is different. Pseudoboehmite formed by synthesis transforms into γ-Al_2O_3 at about 431 °C, and the small exothermic peak on DTA scan at 991 °C (Fig. 2) could be attributed either to γ-Al_2O_3 or to Al–Si spinel (Fig. 3). It is not possible to differentiate Al–Si spinel from γ-Al_2O_3 by XRD analysis, since the both phases not only have similar crystalline structure and close lattice parameters, but also very faint and diffuse XRD peaks with considerable overlapping. If Al–Si spinel instead of γ-Al_2O_3 is formed, the amount of amorphous silica, i.e., the intensity of amorphous hump at about 22° 2θ CuK_α should be decreased and no mullite should be formed. Therefore, the integrated area of the amorphous SiO_2 hump at about 22° 2θ CuK_α and the area of spinel peak at 2θ Cu$K_\alpha = 45.6°$ for the samples heated at 800 °C and 1000 °C, respectively, were compared and given in Fig. 3b. It could be observed that the intensity of the hump belonging to amorphous silica is decreased with temperature. At the same time the intensity of spinel phase is slightly increased and no other crystalline phase was detected. Therefore, the appearance of exotherm at 991 °C on DTA scan is rather attributed to the formation of Al–Si spinel than to γ-Al_2O_3. That is also in accordance with literature.[6] Accordingly, the gel *B* is a combination of type II and type III precursors. That means that above ~990 °C both γ-Al_2O_3, formed by the transformation of pseudoboehmite, and Al–Si spinel, crystallized from SiO_2-rich amorphous matrix, could be present. Both phases react with the rest of amorphous silica forming orthorhombic mullite at 1266 °C.

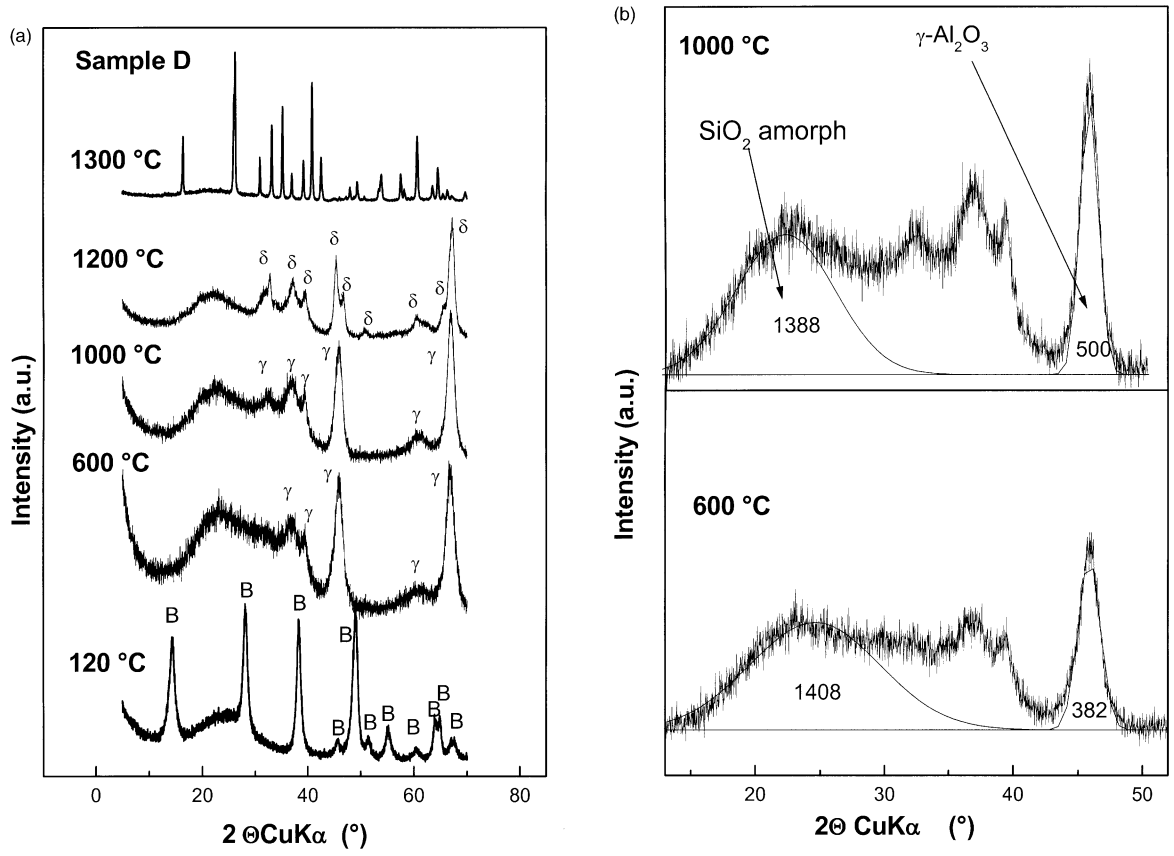

Fig. 5. (a) XRD patterns of the sample *D* heated in DTA up to the temperatures given in the picture. (b) Intensities ratio of amorphous SiO_2 hump at 22° 2θ CuK_α and 400 line of spinel at 2θ 45.6° in the sample heated up to 600 and 1000 °C. Full lines are the best fits to corresponding intensities. γ γ Al_2O_3, δ δ Al_2O_3 and B boehmite. Mullite lines are not marked.

The formation of mullite in samples *C* and *D* and the corresponding DTA scans (Fig. 2) are consistent with the formation of mullite in diphasic type II gels.[2] The gels differentiate from each other only in the crystalline form of alumina component at room temperature. In the gel *C*, it is γ-Al_2O_3 (Fig. 4) and in the gel *D* it is boehmite (Fig. 5), which transforms above 500 °C into γ-Al_2O_3. In both samples, γ-Al_2O_3 added or derived from boehmite reacts with amorphous silica forming orthorhombic mullite above 1300 °C; at 1346 and at 1361 °C, respectively, as shown on DTA scans (Fig. 2). In Fig. 5b, the area below the amorphous silica hump at 22° 2θ CuK_α in the sample *D* was compared with the area of 400 line of γ-Al_2O_3 at 2θ CuK_α = 45.6° for two different temperatures (600 and 1000 °C). The amount of amorphous silica is almost constant in this temperature range, whereas the intensity of γ-Al_2O_3 increases with temperature. It has to be stressed that γ-Al_2O_3 in the sample is formed by decomposition of boehmite and therefore, the formation of Al–Si spinel (i.e., the decrease of amorphous silica) was not expected. Besides, the gels *C* and *D* can be considered as microcomposites with alumina core coated with amorphous SiO_2,[15] what is confirmed by TEM analysis (Fig. 9). Even in samples isothermally sintered at 1320 °C for 4 h the coated amorphous silica has been observed.

4.2. Densification behavior

The dilatometric and corresponding derivative curves of compacts containing aluminium nitrate nonahydrate as a source of alumina (precursors *A* and *B*) show three step of densification (Fig. 6). On the contrary, the compacts *C* and *D* show large densification step between 1000–1300 °C, and the former compact exhibits a small second step at about 1539 °C as well. As shown in Fig. 7, the precursors *B*, *C* and *D* display better densification behavior than the highly amorphous *A* precursor, though in all cases sintering may be controlled by viscous flow mechanism of coexisting SiO_2-rich glass phase.[15] A suitable explanation for the inferior densification behavior of the gel *A* with respect to the other three gels is the lower temperature of mullite formation ($A < 1250$ °C; *C* and $D > 1300$ °C and *B* between 1250 and 1300 °C), which overlaps with the temperature ranges for densification by viscous flow and reaction sintering. The densification of compacts containing γ-Al_2O_3 covered with silica is almost complete prior to mullite crystallization (Fig. 7).

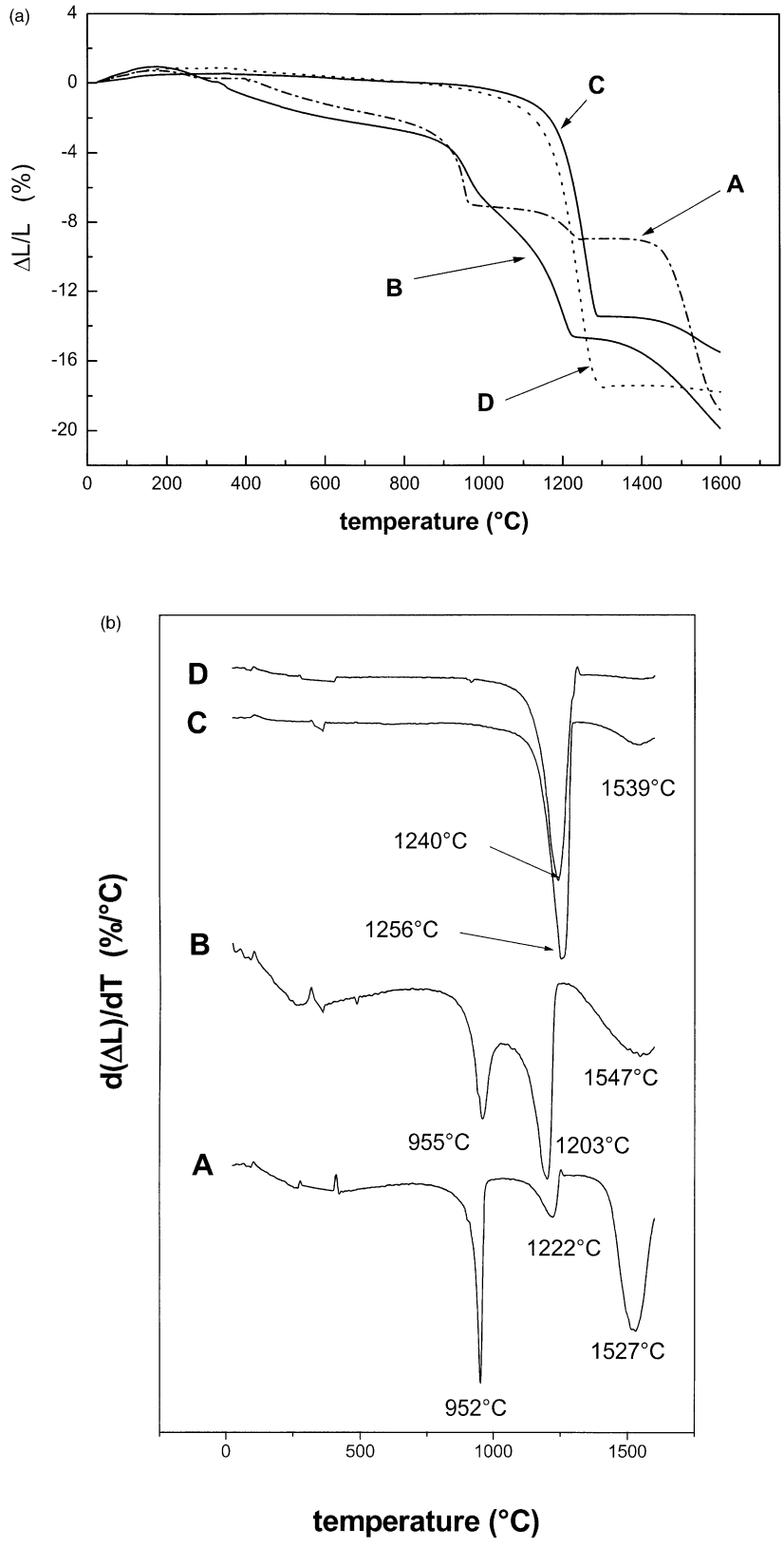

Fig. 6. (a) Dilatometric curves of gels calcined at 700 °C for 9 h. Non isostatic/isostatic pressure 100/200 MPa. (A) diphasic gel (type III), (B) diphasic gel (combination of type III and type II), (C) diphasic gel (type II, γ Al_2O_3); (D) diphasic (type II, boehmite); (b) derivatives of dilatometric curves shown in (a). Heating schedules are described in the text.

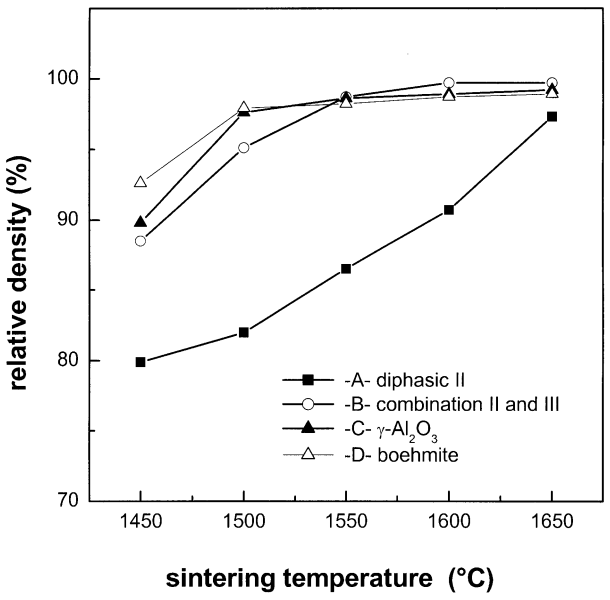

Fig. 7. Density as a function of sintering temperature. Specimen were non isostatic and isostatic pressed at 100/200 MPa and heated at the rate of 5 °C min^{-1} to the sintering temperature. Holding time at each sintering temperature was 2 h. Lines are drawn as guides for the eye.

4.3. Microstructure of sintered compacts

The microstructure evolution in the investigated precursors is largely dependent upon a number of factors (as in any sintering process), including the properties of mullite precursors, calcination conditions, post-calcination treatment and the green body forming method. Except the mullite precursors, all other process conditions were the same in all experiments. Because of that, the differences in the microstructure of the sintered bodies seen in Fig. 8 could be correlated with the properties of precursors, moreover, with the crystalline form and particle size of alumina source in the precursors. It can be assumed that the particle size of amorphous silica in all precursors varies in narrow range, and is smaller than 20 nm, otherwise, according to Fahrenholtz et al.,[12] cristobalite should be formed. No cristobalite was observed in any of the precursors.

The microstructure of samples *A* and *B* (Fig. 8A and B) are characterized by elongated mullite crystals with longer axis about 4–10 μm for the specimen *A* and about 5–7 μm for the specimen *B*, respectively, embedded in a finer "mullite-matrix". The size of smaller

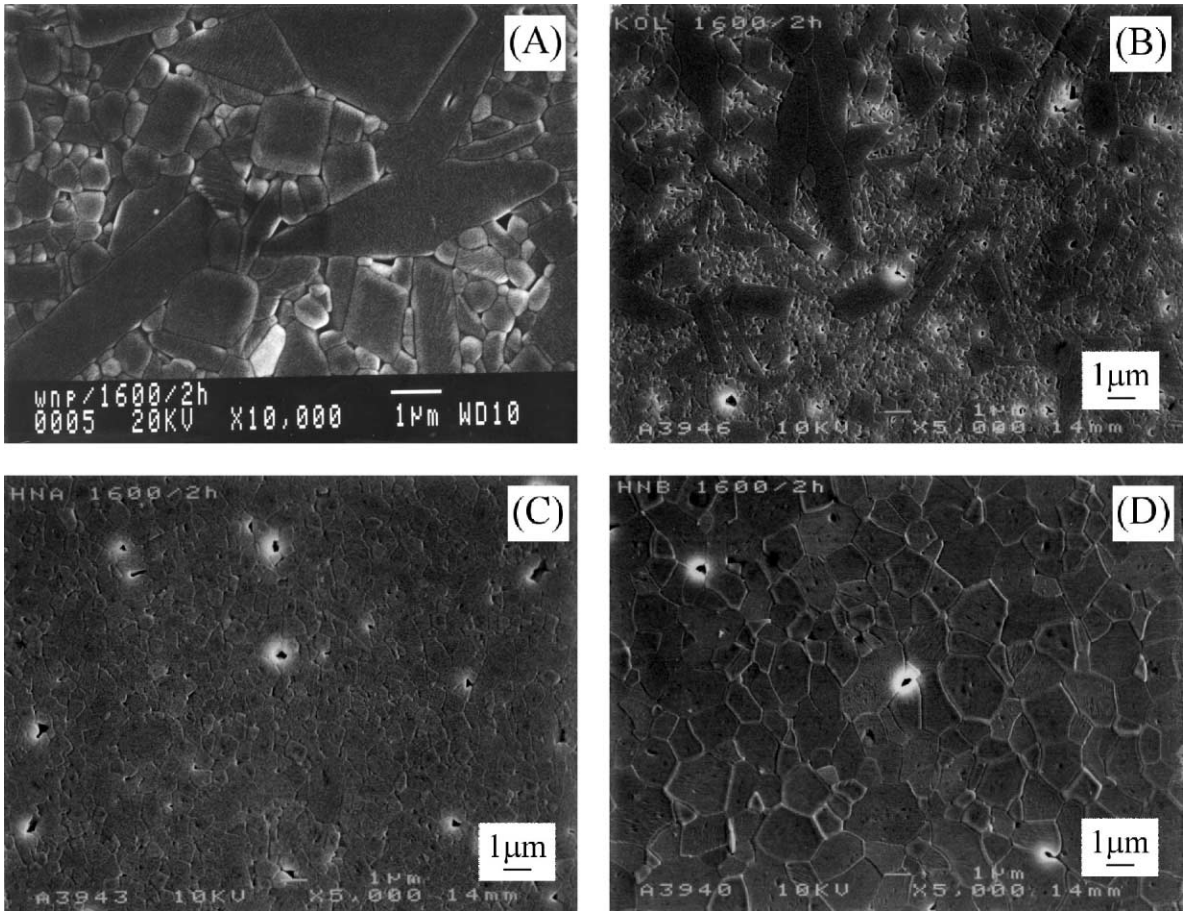

Fig. 8. SEM micrographs of polished and thermally etched pressureless sintered compacts at 1600 °C. (A) the sample *A*; (B) the sample *B*; (C) the sample *C*; and (D) the sample *D*.

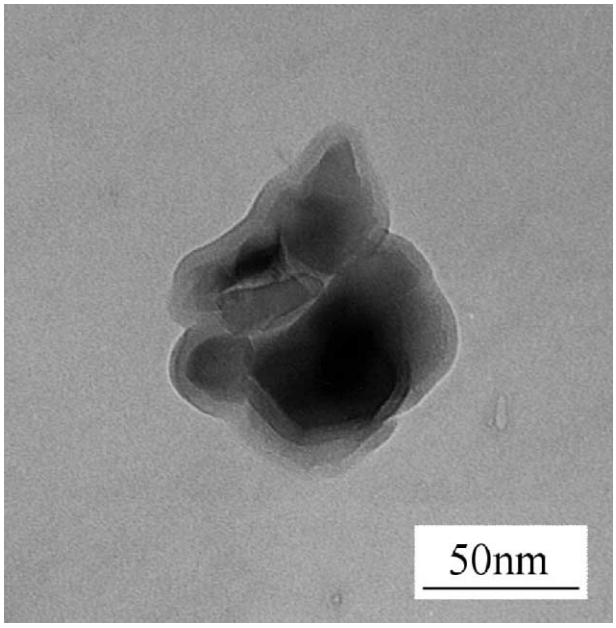

Fig. 9. TEM micrograph of γ Al_2O_3 covered with silica layer. The calcined powder was isothermally sintered at 1320 °C for 4 h.

equaxial "mullite-matrix" crystals was <1 μm, and was larger for the sample *A* and smaller for the sample *B*. The elongated microstructure seen in samples *A* and *B* is similar to that observed by Kanka and Schneider[16] and is attributed to the presence of liquid silica-rich phase. Mullite grains are richer in Al_2O_3 ($Al_2O_3 = 74.2$ wt.%, SiO_2 25.8 wt.%) with respect to 3:2 mullite ($Al_2O_3 = 72.8$ wt.%, SiO_2 28.2 wt.%).

On the contrary, the microstructure of the samples *C* and *D* (Fig. 8C and D) are characterized by equaxial mullite grains with the grains size of 0.5 μm in the former and 1.3 μm in the latter sample. As shown in Fig. 1, the difference of as-prepared gels *C* and *D* is the particle size of alumina used for preparation, being much finer in sample *C*. It is commercial γ-Al_2O_3 with maximum particle sizes of 20 nm in the former, and by decomposition of boehmite formed γ-Al_2O_3 in the latter. Boehmite particle sizes of about 30–40 nm were determined by grain size measurement in TEM dark-field pictures (Fig. 1D). Therefore, no much smaller particle size of γ-Al_2O_3 should be expected. It can be concluded, that the grain size of mullite appears to be governed by the size of alumina component.[17] The finer the alumina particle, the smaller the mullite grain size. The presence of equiaxial grains has generally been associated with the absence of glassy phase and with high alumina compositions,[8,16,18,19] whereas stiff skeleton of interlinked elongated mullite crystals are associated with presence of liquid phase, and stoichiometric or low-alumina compositions.[16]The gels *C* and *D* exhibited stoichiometric 3:2 mullite composition, but the densification of powders was almost complete prior to mullite crystallization as shown in Fig. 6b. Accordingly, our results have shown that equiaxial morphology of mullite grains are not necessarily the effect of high alumina composition, but the shift of mullite crystallization above the sintering temperatures.

5. Conclusion

Clear differences were found in the microstructure of diphasic precursors *A* and *B* in comparison to those of precursors *C* and *D*. Type III gel, and the combination of type II and type III precursors exhibited elongated mullite grains embedded into the "equiaxial mullite matrix". This morphology is due to the overlapping of mullite crystallization and viscous flow sintering temperatures. The inferior densification behavior of gel *A* with respect to the gel *B* is caused by the lower temperature of mullite formation (<1250 °C).

Transient alumina, which is added (sample *C*) or in situ formed (by decomposition of boehmite-sample *D*), covered with amorphous silica shifts the mullite formation above the sintering temperature and enables formation of equiaxial mullite. The smaller are the transient alumina particles, the smaller are mullite grains of sintered bodies.

References

1. Aksay, L. A. and Pask, J. A., Stable and metastable equilibria in the system SiO_2 Al_2O_3. *J. Am. Ceram. Soc.*, 1975, **58**, 507 512.
2. Schneider, H., Voll, D., Saruhan, B., Sanz, J., Schrader, G., Ruscher, C. and Mosset, A., Synthesis and structural character ization of non crystalline mullite precursors. *J. Non Cryst. Sol.*, 1994, **78**, 262 271.
3. Hoffman, D. W., Roy, R. and Komarneni, S., Diphasic xerogels, a new class of materials: phases in the system Al_2O_3 SiO_2. *J. Am. Ceram. Soc.*, 1984, **67**, 468 471.
4. Okada, K. and Otsuka, N., Characterization of spinel phase from SiO_2 Al_2O_3 xerogels and the formation process of mullite. *J. Am. Ceram. Soc.*, 1986, **69**, 652 656.
5. Yoldas, B. E., Mullite formation from aluminium and silicon alkoxides. In *Mullite and Mullite Matrix Composites, Ceramic Transactions, Vol. 6*, ed. S. Somiya, R. F. Davis and J. A. Pask. American Ceramic Society, Westerville, OH, 1990, pp. 255 262.
6. Schneider, H., Voll, D., Saruhan, B. and Schmucker, M., Con stitution of the γ Al_2O_3 phase in chemically produced mullite precursors. *J. Eur. Ceram. Soc.*, 1994, **13**, 441 448.
7. Schneider, H., Okada, K. and Pask, J., *Mullite and Mullite Ceramics*. J. Wiley & Sons, Chichester, 1994, pp. 105 140.
8. Sacks, M. D., Lee, H. W. and Pask, J., A review of powder pre paration methods and densification procedure for fabricating high density mullite. In *Mullite and Mullite Matrix Composites, Ceramic Transactions, Vol. 6*, ed. S. Somiya, R. F. Davis and J. A. Pask. American Ceramic Society, Westerville, OH, 1990, pp. 167 207.
9. Ismail, M. G. M. U., Nakai, Z. and Somiya, S., Sintering of mullite prepared by sol gel method. In *Mullite and Mullite Matrix Composites, Ceramic Transactions, Vol. 6*, ed. S. Somiya, R. F. Davis and J. A. Pask. American Ceramic Society, Wester ville, OH, 1990, pp. 231 241.

10. Komarneni, S., Suwa, Y. and Roy, R., Application of composi tionally diphasic xerogels for enhanced densification: the system Al_2O_3 SiO_2. *J. Am. Ceram. Soc*., 1984, **69**, C155 156.
11. Wei, W. C. and Halloran, J. W., Phase transformation of dipha sic aluminosilicate gels. *J. Am. Ceram. Soc*., 1988, **71**, 581 587.
12. Fahrenholtz, W. G., Smith, D. M. and Cesarano III, J., Effect of precursor particle size on the densification and crystallization behavior of mullite. *J. Am. Ceram. Soc*., 1993, **76**, 433 457.
13. Sacks, M. D., Bozkurt, N. and Scheiffele, G. W., Fabrication of mullite and mullite matrix composites by transient viscous sin tering of composite powders. *J. Am. Ceram. Soc*., 1991, **74**, 2428 2437.
14. Sacks, M. D., Wang, K., Scheiffele, G. W. and Bozkurt, N., Effect of composition on mullitization behavior of α alumina/ silica microcomposite powders. *J. Am. Ceram. Soc*., 1997, **80**, 663 672.
15. Bartsch, M., Saruhan, B., Schmucker, M. and Schneider, H., Novel low temperature processing route of dense mullite cera mics by reaction sintering of amorphous SiO_2 Coated γ Al_2O_3 particle nanocomposites. *J. Am. Ceram. Soc*., 1999, **82**, 1388 1392.
16. Kanka, B. and Schneider, H., Sintering mechanisms and micro structural development of coprecipitated mullite. *J. Mat. Sci*., 1994, **29**, 1239 1249.
17. Kara, F. and Little, J. A., Sintering behaviour of precursor mul lite powders and resultant microstructures. *J. Eur. Ceram. Soc*., 1996, **16**, 627 635.
18. Kara, F. and Little, J. A., Sintering of premullite obtained by chemical processing. *J. Mat. Sci*., 1993, **28**, 1323 1326.
19. Kara, F. and Şener, O., Improvement of sintering and micro structural homogeneity of diphasic mullite. *J. Eur. Ceram. Soc*., 2001, **21**, 901 905.